Eur. Phys. J. B **34**, 399–407 (2003)
DOI: 10.1140/epjb/e2003-00237-9

THE EUROPEAN PHYSICAL JOURNAL B

Heavy fermions in transition metals and transition-metal oxides

H.-A. Krug von Nidda[1], R. Bulla[2], N. Büttgen[1,a], M. Heinrich[1], and A. Loidl[1]

[1] Experimentalphysik V, Elektronische Korrelationen und Magnetismus, Institut für Physik, Universität Augsburg, 86135 Augsburg, Germany
[2] Theoretische Physik III, Elektronische Korrelationen und Magnetismus, Institut für Physik, Universität Augsburg, 86135 Augsburg, Germany

Received 15 May 2003
Published online 9 September 2003 –

Abstract. Heavy–fermion formation in transition metals and transition–metal oxides is reviewed and compared to observations in canonical f–derived heavy–fermion systems. The work focuses on the dynamic susceptibilities which reveal a characteristic temperature and frequency dependence and which can be unambiguously determined *via* nuclear magnetic resonance and electron–spin resonance measurements as well as *via* quasielastic neutron–scattering studies. Different routes to heavy–fermion behaviour are discussed, amongst them Kondo systems, frustrated magnets, and electronically correlated systems close to a metal–insulator transition. From a theoretical point of view, utilizing dynamical mean–field theory, we show that dynamic susceptibilities as calculated for the Hubbard model and for the periodic Anderson model look qualitatively rather similar. These different theoretical concepts describe an universal behaviour of the temperature dependent dynamic susceptibility.

PACS. 71.27.+a Strongly correlated electron systems; heavy fermions – 71.30.+h Metal-insulator transitions and other electronic transitions – 76.60.-k Nuclear magnetic resonance and relaxation – 76.30.Kg Rare-earth ions and impurities

1 Introduction

Since the discovery of an enormously enhanced linear term of the heat capacity $C = \gamma T$, with $\gamma = 1620$ mJ/(mol K^2) and a concomitantly enhanced Pauli–like spin susceptibility ($\chi_0 = 0.036$ emu/mol) in $CeAl_3$ [1], strongly correlated electron systems with a quasi–particle mass enhancement of $m^*/m \approx 10^2 - 10^3$ are in the focus of solid–state physics. While in the early times mainly $4f$- and $5f$-derived heavy fermions like the heavy–fermion superconductor $CeCu_2Si_2$ [2] were investigated, the main interest recently turned towards transition metals and transition–metal oxides also revealing strongly enhanced Sommerfeld coefficients γ and spin susceptibilities χ_0. Recent examples are Sc doped YMn_2 [3,4] and LiV_2O_4 [5–7]. These $3d$–metals compounds are Fermi liquids, with an enhanced linear term of the heat capacity, and an enhanced almost constant susceptibility towards low temperatures. In addition, the resistivity ρ is dominated by electron–electron interactions yielding a quadratic temperature dependence $\rho = A \times T^2$ with A satisfying the Kadowaki–Woods relation [8], $A/\gamma^2 = 10^{-5}\ \mu\Omega\,\mathrm{cm/K^2}$ which holds for a variety of strongly correlated Fermi liquids. At the same time the Wilson ratio, $R_W = (\pi^2 k_B^2/3\mu_B^2\mu_0) \times \chi_0/\gamma$ [9,10] is between 1 and 2, again characteristic for correlated electron systems. The Wilson ratio is thought to distinguish the enhancement of γ resulting from spin fluctuations *via* the Stoner mechanism, from the regular mass enhancement due to a high electron density of states. And while all of these compounds show the characteristics of heavy Fermi liquids, it is clear that the routes to the formation of heavy quasi–particle masses must be very different.

It is the aim of the present investigation to study this heavy–fermion formation in d–metals and transition–metal oxides in more detail. For this purpose we focus on the dynamic susceptibility which reveals a characteristic temperature dependence and can be directly studied employing inelastic neutron scattering (INS), electron–spin resonance (ESR) and nuclear magnetic resonance (NMR) techniques. Experimental results on a variety of systems are reviewed and compared with recent theoretical investigations. Thereby we want to work out universalities in the heavy–fermion formation but also to find differences which allow to classify different classes of compounds. Different scenarios of heavy–fermion behaviour have previously been discussed by Fulde [11]. In that work Kondo lattices, localized spins in a sea of strongly correlated electrons, and examples of charge–ordering systems have been discussed.

After briefly reviewing the main observations in canonical f–derived heavy–fermion systems we shall discuss a

[a] e-mail: norbert.buettgen@physik.uni-augsburg.de

Table 1. Compounds with enhanced Sommerfeld coefficients γ and enhanced Pauli spin susceptibilities χ_0 (SI values in m^3/mol are obtained after multiplying χ_0 by $4\pi \times 10^{-6}$). Here all systems are listed which reveal a Sommerfeld coefficient larger than 39 mJ/(mol K^2). For $Gd_{0.8}Sr_{0.2}TiO_3$, the susceptibility χ_0 is not determined (nd) because the dominant Curie–type contribution of the Gd–Spins masks the Pauli spin susceptibility. The route to heavy–fermion formation is indicated originating from magnetic frustration (F), Kondo–lattice behaviour (KL), quantum critical point (QCP), or metal–to–insulator transition (MIT), respectively. The question mark denotes conflicting statements in the literature (see text).

	γ(mJ/(mol K^2))	$\chi_0(\times 10^{-3}$ emu/mol)	Character	Reference
LiV_2O_4	490	11	F/KL (?)	(Brando *et al.* 2002) [7]
LiV_2O_4	350	9	F/KL (?)	(Urano *et al.* 2001) [6]
Y(Sc)Mn_2	160	1.4	F	(Nakamura 1988) [4]
$CaRuO_3$	77	0.7	QCP/MIT (?)	(Cao *et al.* 1997) [41]
β-Mn	70	0.5	F	(Nakamura *et al.* 1997) [37]
$Gd_{0.8}Sr_{0.2}TiO_3$	50	nd	MIT	(Heinrich *et al.* 2002) [22]
Sr_2RuO_4	39	0.97	MIT/QCP (?)	(Maeno *et al.* 1994) [42]

number of d–metals or transition–metal oxides which can be grouped into different schemes. The formation of heavy fermions seems to be a common feature to systems with strong spin fluctuations, *i.e.* Kondo–lattice compounds (KL), systems close to a metal–to–insulator transition (MIT), frustrated magnets (F), and materials in the vicinity of a quantum critical point (QCP). Table 1 lists some compounds which can be grouped using these classifications and will be studied in detail in this paper. All of these compounds are highly correlated Fermi liquids with a T^2 temperature dependence of the resistivity, an enhanced Sommerfeld coefficient, and an enhanced Pauli–like spin susceptibility. Figure 1 shows the Wilson ratio R_W *versus* the magnetic susceptibility on a double–logarithmic plot. The free–electron gas has a Wilson ratio $R_W = 1$, an isolated Kondo ion yields $R_W = 2$, correlated metals are expected between $1 \leq R_W \leq 2$, and the Brinkman–Rice–Gutzwiller spin liquid gives $R_W = 4$ [12]. Values of the Wilson ratio above 2 have also been found in calculations for the Hubbard model [13]. And indeed, all compounds documented in Figure 1 reveal values between 0.5 and 4. Values smaller than 1 are expected, if the Landau Fermi–liquid parameter is negative. It is interesting to note that there exists a clear correlation in the data shown in Figure 1: the larger the susceptibility χ_0 the larger the Wilson ratio R_W.

Experimental results for these compounds are described in detail in Section 2. Section 3 introduces a theoretical approach for the microscopic understanding of the spin dynamics of Kondo lattices and systems close to a Mott transition. The paper is summarized in Section 4.

2 Experimental results

In this section, we give an overview on results in transition metals and transition–metal oxides obtained in our laboratory, but we also refer to published work. Before doing so, we briefly discuss the heavy–fermion formation in canonical f–derived compounds.

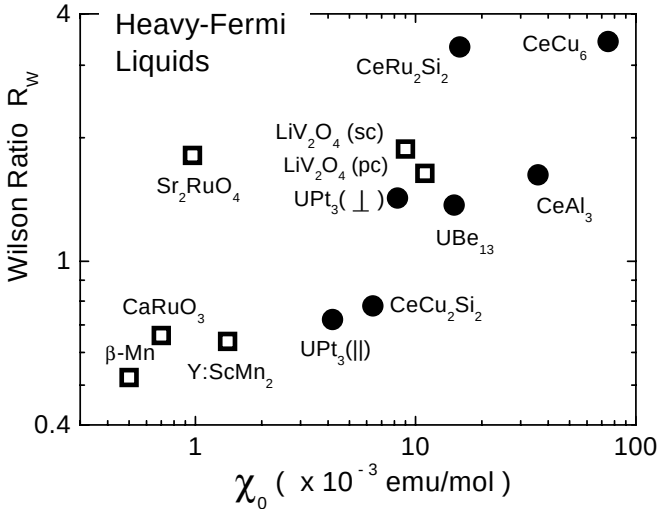

Fig. 1. Wilson Ratio *versus* susceptibility. Open and solid symbols denote d– and f–derived compounds, respectively. pc: polycrystal, sc: single crystal. For the susceptibility data of UPt_3 the directions of the magnetic field with respect to uniaxial crystal symmetry are indicated [15].

2.1 Kondo lattices

In $4f$– and $5f$–derived compounds, experimental work has been performed for almost 30 years and an incredible amount of data is available, most of which is reviewed in the work by Stewart [14], Ott [10], and Grewe and Steglich [15]. In Kondo lattices an enormously enhanced effective mass results from an interplay between the local Coulomb repulsion within the f–states and the hybridization between f– and band states. At high temperatures the local moments are not screened yielding a Curie–Weiss–like paramagnetism. However, below a characteristic temperature T^* the local moments of the f–shell are quenched and a heavy Fermi liquid with a strongly enhanced linear term of the heat capacity and a concomitantly enhanced Pauli spin susceptibility is formed. It is the general believe that spin fluctuations are responsible for the collective compensation of the local moments.

Dynamic susceptibilities in Kondo compensated heavy fermions have been studied in detail by neutron scattering [16], NMR [17] and ESR techniques [18]. The fluctuation–dissipation theorem provides the important relation between the imaginary part of the dynamic susceptibility $\chi_f(\mathbf{Q},\omega,T)$ and the fluctuating magnetization $M_f(\mathbf{Q},t)$ of the Kondo ions.

$$\frac{1}{2}\int_{-\infty}^{+\infty}\langle M_f(\mathbf{Q},0)M_f(\mathbf{Q},t)\rangle_T \exp(i\omega t)\mathrm{d}t = \frac{\mathrm{Im}\chi_f(\mathbf{Q},\omega,T)}{1-\exp(-\hbar\omega/k_\mathrm{B}T)}. \quad (1)$$

On the right–hand side, the term $[1-\exp(-\hbar\omega/k_\mathrm{B}T)]^{-1}$ is the detailed–balance factor. The left–hand side is the Fourier–transformed thermal average of the magnetization–correlation function $\langle ...\rangle_T$, which is proportional to the dynamic structure factor $S(\mathbf{Q},\omega,T)$ measured by quasi–elastic neutron scattering (QNS) at momentum transfer $\mathbf{Q}$ and energy transfer $\hbar\omega$ [16].

The dynamic susceptibility can be measured not only *via* the dynamic structure factor $S(\mathbf{Q},\omega,T)$ in neutron–scattering experiments, but also *via* the spin-lattice relaxation rate $1/T_1$ in NMR experiments and *via* the linewidth ΔH at resonance absorption using ESR techniques. NMR probes the spin–lattice relaxation rate $(1/T_1)_\mathrm{NMR}$ of an appropriate nuclear spin in the neighbourhood of the Kondo ion. ESR measures the resonance linewidth ΔH_ESR of a paramagnetic ion with a stable magnetic moment (*e.g.* Gd^{3+} in the systems discussed here), a few percent of which has to be doped into the Kondo–lattice compound, because the spins of the Kondo ions fluctuate too fast to give a detectable ESR signal. The ESR linewidth represents the transversal spin–relaxation rate $(1/T_2)_\mathrm{ESR}$ of the ESR probe which in metals equals the longitudinal or spin–lattice relaxation rate $(1/T_1)_\mathrm{ESR}$. The dynamic susceptibility of the Kondo ion is transferred to NMR and ESR probes by RKKY–like indirect exchange interactions *via* the conduction electrons. Hence NMR relaxation rate $(1/T_1)_\mathrm{NMR}$ and ESR linewidth ΔH_ESR can be related to the dynamic structure factor $S(\mathbf{Q},\omega,T)$ of QNS in the high–temperature approximation ($k_\mathrm{B}T \gg \hbar\omega$) and neglecting the $\mathbf{Q}$ dependence [19]:

$$S(\omega,T) \propto \frac{T}{\omega}\mathrm{Im}\chi_f(\omega,T) \propto (1/T_1)_\mathrm{NMR} \propto \Delta H_\mathrm{ESR}. \quad (2)$$

From an experimental point of view, the frequency dependence of the dynamic susceptibility can be described using a purely relaxational ansatz for the correlation function in equation (1). Then the imaginary part of the dynamic susceptibility is of Lorentz shape centered at $\omega = 0$,

$$\mathrm{Im}\chi_f(\omega,T) = \frac{\omega\Gamma}{\omega^2+\Gamma^2}\chi_{stat} \overset{\Gamma\gg\omega}{\longrightarrow} \frac{\omega}{\Gamma}\chi_{stat} \quad (3)$$

with the magnetic relaxation rate Γ (= quasi–elastic linewidth) and the static susceptibility χ_{stat} of the Kondo ions. Of course, in QNS experiments the dynamic susceptibility can be studied as a function of temperature and within a very broad frequency range, whereas NMR and ESR are always working at fixed frequency ω_0 in the MHz to GHz range, respectively. This corresponds to the low-energy transfer limit indicated on the right–hand side of equation (3), because the experimental frequencies are small compared to the quasi–elastic linewidth which is of the order of the characteristic temperature T^*.

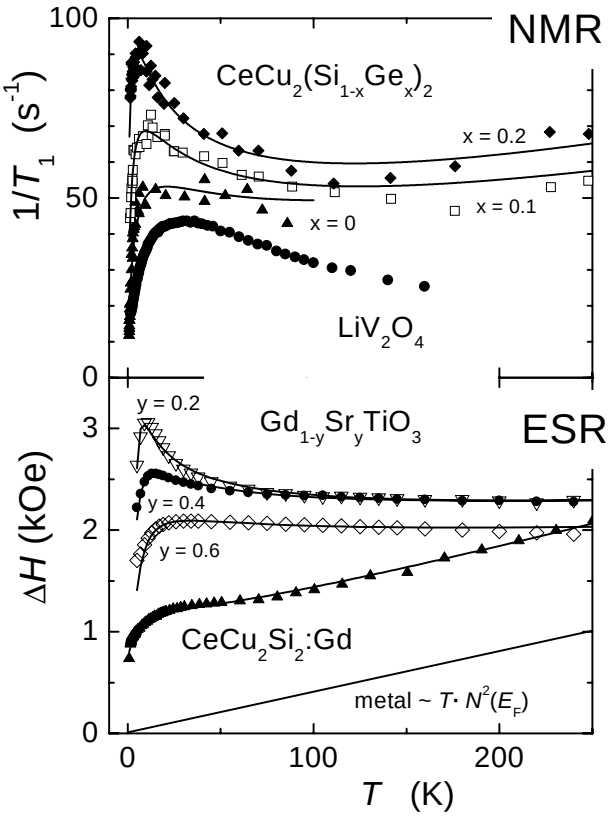

Fig. 2. Temperature dependence of the NMR relaxation rate $1/T_1$ of ^{63}Cu and ESR linewidth ΔH in $CeCu_2(Si_{1-x}Ge_x)_2$, respectively (NMR data of $CeCu_2Si_2$ are taken from Asayama [17]; ESR data obtained after doping with 1% Gd^{3+} at the Ce site). Additionally, $1/T_1$ of ^{7}Li in LiV_2O_4 and ΔH of Gd^{3+} ESR in $Gd_{1-y}Sr_yTiO_3$ are shown. The solid lines are fits which are described explicitly in references [22,24] (see Sect. 2.2).

In a typical heavy–fermion compound at temperatures $T \ll T^*$, the spins of the Kondo ions are completely screened by the conduction electrons; a large Pauli–like susceptibility $\chi_0 = \text{const.}$ and a large, temperature independent relaxation rate $\Gamma \approx T^*$ yield a strongly enhanced Korringa–like increase of expression (2) with temperature. This is followed by a decrease at temperatures $T > T^*$, where the static susceptibility follows a Curie–Weiss law $\chi_{stat} \propto (T+\alpha T^*)^{-1}$ with $\alpha = \sqrt{2}$ [20] and the relaxation rate Γ increases according to $\Gamma \propto \sqrt{T}$ [21].

Figure 2 shows $1/T_1$ as observed in the heavy–fermion superconductor $CeCu_2Si_2$ [17] and in $CeCu_2(Si_{1-x}Ge_x)_2$ (upper frame), and ΔH as observed *via* Gd–ESR in $CeCu_2Si_2$ (lower frame). These results, which are typical for f–derived Kondo-lattices, are compared to the

temperature dependence of the spin–lattice relaxation rate in LiV_2O_4 [7], which has been termed the first d–derived heavy–fermion metal [5], and to the ESR linewidth at resonance absorption in $Gd_{1-y}Sr_yTiO_3$ [22] for different concentrations on the metallic side of the metal–to–insulator transition. Starting from high temperatures, all compounds investigated show a Curie–Weiss type increase towards lower temperatures, a maximum at the characteristic temperature T^* and a linear Korringa–type relaxation at lowest temperatures. This behaviour is exactly what is expected within the ansatz outlined above. To describe the NMR and ESR data for the $4f$-derived compound $CeCu_2(Si_{1-x}Ge_x)_2$, an additional linear Korringa term was added to equation (3). Such a term is due to the direct relaxation contribution of the conduction electrons [23] and is observed in all metals (indicated at the bottom of Fig. 2). Its slope is proportional to the squared electronic density of states at the Fermi level $N^2(E_F)$. The different ratio of the direct Korringa contribution and the Kondo fluctuations observed for ESR and NMR reflects the strong dependence of the RKKY interaction on the distance between the magnetic resonance probe and the Kondo ions [24]. This result underlined the local character of the hybridization in canonical f–derived Kondo lattices. The fit curves for $Gd_{1-y}Sr_yTiO_3$ were calculated using the phenomenological spin–fluctuation model by Ishigaki and Moriya [25,26] which will be described in the following subsection.

2.2 Heavy fermions at the metal–to–insulator transition

The critical behaviour of the electronic specific heat close to a MIT is experimentally well established. Well known examples are doped $LaTiO_3$ and $YTiO_3$ [27]. These compounds are just on the insulating side of the Mott–Hubbard transition and a MIT can easily be induced by doping small amounts of Sr or Ca. Recently, the critical increase of the Sommerfeld coefficient at the MIT has also been detected in Sr-doped $GdTiO_3$ [22]. Pure $GdTiO_3$ is a ferrimagnetic Mott insulator. A metallic ground state is induced on substituting 20% of Gd by Sr. On approaching the MIT from the metallic side the Sommerfeld coefficient strongly increases reaching values of almost 60 $mJ/(mol\,K^2)$ [22]. The dynamic susceptibility of this system has been studied using Gd–ESR at X-band frequency [22]. Some representative results of the linewidth ΔH within the metallic regime $0.2 \leq y \leq 0.6$ are shown in the lower frame of Figure 2. Starting at low temperatures the linewidth increases linearly, passes through a maximum close to the characteristic temperature T^*, and reveals a Curie-Weiss like behaviour at higher temperatures. Approaching the MIT from the metallic side ($y \geq 0.2$), the prominent maximum in $\Delta H(T)$ increases and shifts to lower temperatures T^*. This behaviour strongly resembles the relaxation contribution of the Kondo ions in the typical heavy–fermion compounds. Instead of the Kondo f–ions, the Ti^{3+} ($3d$) spin system exhibits fluctuations which are transferred to the Gd spin *via* super–exchange interactions. For an appropriate description of the dynamic susceptibility the itinerant character of the Ti electrons has to be taken into account, following Ishigaki and Moriya [26], who developed a theoretical description of nuclear magnetic relaxation around the magnetic instabilities in metals. Their results were used to explain the NMR relaxation rate in $Ca_{1-x}Sr_xRuO_3$ [28] discussed below and have been modified for the ESR results in $Gd_{1-y}Sr_yTiO_3$ as described in reference [22]. Inserting this dynamic susceptibility in equation (2) yields for the ESR linewidth

$$\Delta H \propto \frac{3Ty^2}{2(y^3+h)}. \tag{4}$$

The reduced inverse $3d$ susceptibility y is given by an implicit integral equation [26], which has to be iterated numerically. Its two characteristic parameters are correlated with the inverse static susceptibility at zero temperature and the energy width of the dynamical spin–fluctuation spectrum. The parameter $h \propto H^2$ accounts for the influence of the applied magnetic field H. The resulting fit curves are drawn as solid lines in the lower frame of Figure 2. In Section 3 we show that the characteristic temperature dependence of the dynamic susceptibility can also be obtained qualitatively using microscopic models.

2.3 Heavy–fermion formation in frustrated magnets

Frustrated magnets are systems which cannot minimize simultaneously all the pairwise magnetic interactions due to geometrical constraints. In three dimensions, pyrochlores are good examples of frustrated magnets. They reveal exotic ground states like spin liquids or spin–ice states [29]. In pyrochlores, local spins with antiferromagnetic (AFM) interactions are located on ideal tetrahedral lattice sites. Due to geometrical constraints long–range magnetic order (strictly speaking only Ising spins with AFM nearest neighbour interactions are frustrated) is suppressed and in some compounds the Curie-Weiss behaviour can be observed down to the lowest temperatures. LiV_2O_4 and $Y(Sc)Mn_2$ exhibit an ideal tetrahedral arrangement of the $3d$ spins. In the case of lithium–vanadate it is believed that one vanadium t_{2g} electron per lattice site forms a localized moment, while 0.5 electrons per site represent the band states. Both compounds reveal very high Sommerfeld coefficients of the specific heat, reaching approximately 0.5 $J/(mol\,K^2)$ for LiV_2O_4 [5–7] and 0.16 $J/(mol\,K^2)$ for $Y(Sc)Mn_2$ [3]. While $Y(Sc)Mn_2$ was treated as frustrated magnet from the very beginning, LiV_2O_4 has also been explained as Kondo-compensated heavy–fermion system, where the spin of the local moment is screened by the band states [30]. The significant difference to f–derived heavy fermions certainly is that both the localized moments and the conduction electrons are derived from the vanadium d–states. However, many authors view the magnetic frustration as important ingredient of the heavy–fermion formation [31–36].

The temperature dependence of the dynamic susceptibility as measured *via* the ^7Li spin–lattice relaxation [7]

is shown in Figure 2 and compared to the Cu–NMR results of pure and Ge-doped $CeCu_2Si_2$ where the maximum temperature T_{max} in the temperature dependence of $1/T_1(T)$ turns out to give the characteristic temperature T^* ($T_{max} \approx T^*$). This typical temperature dependence can be explained assuming a Curie–Weiss type susceptibility with a non–zero Curie–Weiss temperature and a weakly temperature dependent magnetic relaxation rate Γ [19]. Such a weak temperature dependence of Γ is typical for frustrated magnets [37], whereas in the case of Kondo lattices it is only constant below T^* but follows a square–root behaviour $\Gamma(T) \propto \sqrt{T}$ at elevated temperatures [21]. At this point we would like to state that this temperature dependence of the dynamic susceptibility can also well be fitted using Moriya's spin–fluctuation theory [25]. And already very early Fujiwara *et al.* described $1/T_1(T)$ in LiV_2O_4 using this approach [38].

A further example of a frustrated magnet with heavy–fermion formation is β–Mn with a Sommerfeld coefficient of 70 mJ/(mol K^2) and a static susceptibility $\chi_0 = 0.5 \times 10^{-3}$ emu/mol [37]. β-Mn, which easily can be obtained by quenching, does not reveal magnetic order down to the lowest temperatures and has been characterized as a spin liquid due to geometrical frustration [37]. A number of NMR experiments have been conducted in $\beta-$Mn [37,39]. As there are two crystallographically inequivalent sites, the ^{55}Mn spin–lattice relaxation rate $1/T_1$ has been measured at both sites. $1/T_1(T)$ as obtained at site II revealed a square–root dependence on temperature for temperatures 3 K $\leq T \leq$ 150 K [39]. In the framework of Moriya's spin–fluctuation theory [26], this experimental observation was taken as an indication that β–Mn is close to an AFM quantum–critical point (QCP). Later on the spin–lattice relaxation of site I has been investigated for temperatures 2 K $\leq T \leq$ 100 K [37]. The overall temperature dependence of $1/T_1$ looks very similar to the examples displayed in Figure 2. However, below 40 K the results have been parameterized using a square–root dependence of the relaxation rate on temperature [37], indicative for a system close to an AFM quantum–critical point. Very recently, non–Fermi liquid effects were also observed in the temperature dependence of the electrical resistivity, with $\rho \sim T^{3/2}$, again corresponding to a nearly AFM metal [40].

2.4 Further *d*-derived heavy fermions

A number of further heavy–fermion liquids have been observed in transition–metal oxides. For example, $Sr_{1-x}Ca_xRuO_3$ has been investigated in detail by Yoshimura *et al.* [28] using ^{17}O NMR. $SrRuO_3$ is an itinerant ferromagnet with a magnetic ordering temperature $T_c = 160$ K. $CaRuO_3$ is a highly correlated non–magnetic metal characterized by a Sommerfeld coefficient of 73 mJ/(mol K^2) [41]. It is assumed that $CaRuO_3$ is close to a ferromagnetic (FM) QCP. On doping Ca into $SrRuO_3$ ferromagnetism is suppressed close to $x = 0.7$. The temperature dependencies of the ^{17}O spin-lattice relaxation rate in $Sr_{1-x}Ca_xRuO_3$ have been measured for Ca concentrations $x = 1$, 0.6 and 0. In pure $SrRuO_3$, $1/T_1$ reveals a peak–shaped anomaly at the FM phase transition. However, for $x = 0.6$ and $x = 1$ the spin–lattice relaxation rate $1/T_1(T)$ resembles the characteristics of heavy fermions like the systems which are displayed in Figure 2. For both compounds, the characteristic temperatures as determined by the maximum in $1/T_1(T)$ is high and close to or even above room temperature. Again, utilizing the spin–fluctuation theory [26] the experimental results for $x = 0.6$ and 1 were reasonably described assuming the systems close to a FM instability [28].

Finally, it is worth to mention the layered perovskite Sr_2RuO_4 which probably reveals triplet–superconductivity below 1.5 K [42]. Sr_2RuO_4 is an almost two–dimensional Fermi liquid with a Sommerfeld coefficient of 39 mJ/(mol K^2) and an enhanced spin susceptility of 0.97×10^{-3} emu/mol [43]. In neutron–scattering studies it has been demonstrated that the relaxation rate Γ of the generalized susceptibility reveals a large residual value of 8 meV, which is a measure of the characteristic temperature T^* of the system. Measurements of the nuclear spin–lattice relaxation rate $1/T_1$ at the planar O(1) site and at the Ru site have been performed by Imai *et al.* [44] for temperatures 2 K $\leq T \leq$ 500 K. Both temperature dependencies reveal the characteristics of the dynamic susceptibility of strongly correlated electron systems and a characteristic temperature of $T^* = 80$ K has been determined in good agreement with the neutron–scattering result. The mechanism for the enhancement of the quasi–particle masses is unclear at present. However, Sr_2RuO_4 is very close to magnetic order and to a MIT [45,46]. So, a QCP as well as a MIT could be the underlying mechanism for the heavy–fermion formation.

3 Theory for the dynamic spin susceptibility

It is evident from the discussion in Section 2 that the different routes to heavy–fermion behaviour also require the use of different theoretical concepts. In some of the above cases it is not even clear which microscopic model should be used for a given material. An example which has been intensively discussed recently is LiV_2O_4, for which a number of different scenarios have been put forward [30–36].

Here we do not want to give a detailed overview of the theoretical approaches for all the routes discussed above. Instead we describe an approach, relevant for the heavy–fermion formation in 2.1 and 2.2, which gives direct information on the full frequency dependence of the dynamic susceptibility. This allows to reproduce qualitatively the temperature dependence of relaxation rate and linewidth in Kondo lattices and also the doping dependence in the case of $Gd_{1-y}Sr_yTiO_3$.

Let us start with the Hubbard model [47] as a microscopic model for the Mott-transition in $Gd_{1-y}Sr_yTiO_3$

$$H = -t \sum_{\langle ij \rangle \sigma} \left(c^\dagger_{i\sigma} c_{j\sigma} + c^\dagger_{j\sigma} c_{i\sigma} \right) + U \sum_i c^\dagger_{i\uparrow} c_{i\uparrow} c^\dagger_{i\downarrow} c_{i\downarrow}. \quad (5)$$

In the model (5), $c^\dagger_{i\sigma}$ ($c_{i\sigma}$) denote creation (annihilation) operators for a fermion on site i with spin σ up ($\uparrow$) or down ($\downarrow$), t is the hopping matrix element and the sum $\sum_{\langle ij\rangle}$ is restricted to nearest neighbours. The second term in (5) describes the local Coulomb repulsion U between two electrons on the same lattice site.

The single-band Hubbard model (5) is certainly too simplified to describe all the physics of the transition-metal oxide $Gd_{1-y}Sr_yTiO_3$ quantitatively. Nevertheless, we expect a reasonable qualitative description of the physics close to the Mott-transition within this model.

Our aim is to calculate the frequency, temperature, and doping dependence of the dynamical spin susceptibility

$$\chi(\omega) = i \int_0^\infty \mathrm{d}t\, e^{i\omega t} \langle [S^z(t), S^z(0)] \rangle \cdot \qquad (6)$$

Here we show calculations performed within the framework of the dynamical mean–field theory [13] (DMFT). In this method, the electronic self–energy $\Sigma(\omega)$ is approximated to be purely local, *i.e.*, k-independent. The DMFT gets exact in the limit of infinite dimensions [48] and is believed to be a good approximation also for real three-dimensional systems [13].

Within the DMFT, the self-energy of a lattice model is calculated from an effective single–impurity Anderson model

$$H = \sum_\sigma \varepsilon_\mathrm{f} f^\dagger_\sigma f_\sigma + U f^\dagger_\uparrow f_\uparrow f^\dagger_\downarrow f_\downarrow + \sum_{k\sigma} \varepsilon_k c^\dagger_{k\sigma} c_{k\sigma} + \sum_{k\sigma} V \left(f^\dagger_\sigma c_{k\sigma} + c^\dagger_{k\sigma} f_\sigma \right). \qquad (7)$$

The operators $f^{(\dagger)}_\sigma$ correspond to the fermionic operators of a given site of the Hubbard model, while the surrounding medium is reduced to a *dynamic* mean field given by the effective conduction band operators $c^{(\dagger)}_{k\sigma}$. The effective bath has to be determined self–consistently [13] which also defines the parameter V and the dispersion ε_k in (7).

The calculation of $\Sigma(\omega)$ for the model (7) is a very difficult many–body problem [13,20]. Recently, it has been shown that the numerical renormalization–group method (NRG), developed by Wilson for the Kondo problem [9,49], is a very powerful tool also for the effective impurity model within the DMFT [50,51]. The NRG is non-perturbative and can access arbitrarily small energy scales — which is essential for the description of systems with characteristic temperature scales of the order of 10 K and below.

Technical details for the application of the NRG to the Hubbard model and the periodic Anderson model have been described in references [50,51]. After convergence of the self-consistency cycle has been reached, the local spin–susceptibility is calculated using the converged effective single–impurity Anderson model. This quantity has previously been calculated for the doped Hubbard model using the quantum Monte–Carlo approach [52]. The focus of reference [52], however, was on the intermediate temperature behaviour of the NMR relaxation rate, which shows striking similarity to the one observed in the High–T_c–compounds.

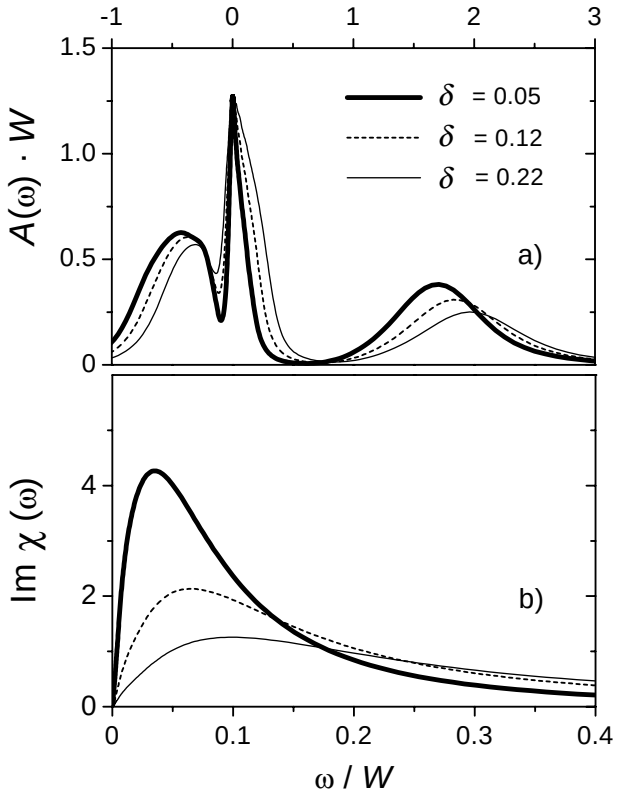

Fig. 3. a) Zero-temperature spectral function for the Hubbard model with $U/W = 2.0$ and different dopings ($\delta = 0$ corresponds to half–filling); b) imaginary part of the spin susceptibility Im $\chi(\omega)$ for the same parameters as in a).

Let us first consider the results for the Hubbard model equation (5). A semi–elliptic density of states is used for the uncorrelated system and the Coulomb repulsion is set to $U = 2\ W$ (W: bandwidth). For this value of U, the system undergoes a metal–insulator transition, when the system approaches half–filling ($n \to 1$). This filling–induced metal–insulator transition is similar in character as the transition observed in $Gd_{1-y}Sr_yTiO_3$; although the transition there occurs at a *finite* value of the doping $\delta \approx 0.1$.

Typical results for the spectral function are shown in Figure 3a for dopings $\delta = 0.05, 0.12, 0.22$ and temperature $T = 0$. Upon decreasing the doping, the lower Hubbard band moves away from the chemical potential and the width of the quasiparticle peak decreases significantly. This corresponds to the enhancement of the effective mass on approaching the MIT. Note also that the increase of the effective mass m^* is not associated with an increase of the density of states at the Fermi level (the linear dependence $m^* \propto N(E_\mathrm{F})$ only holds in the non-interacting case). In the case of interacting electrons studied here, the increase in the specific heat coefficient γ (and hence the increase in m^*) can be understood from the temperature evolution of the spectral function. Upon increasing the temperature up to, let's say, ten times the low-temperature scale T^*, the quasi–particle peak is almost completely destroyed (see

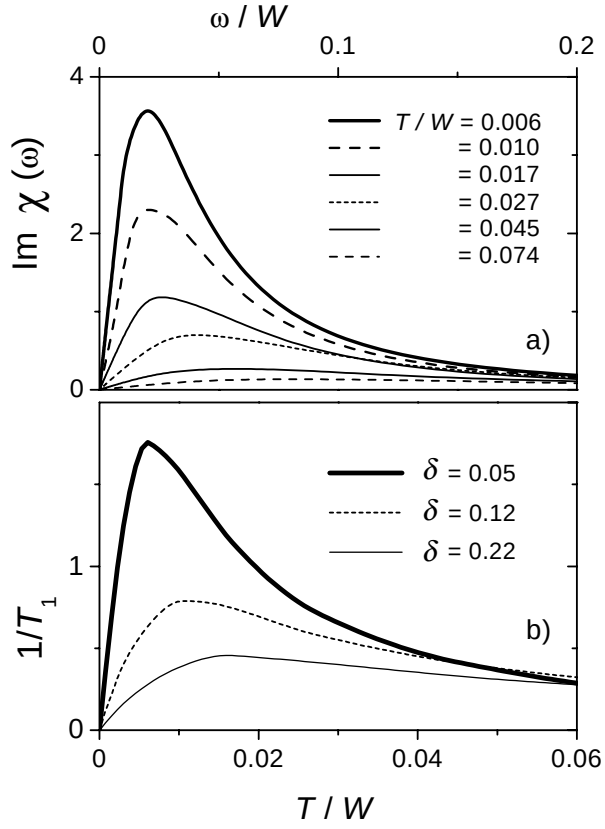

Fig. 4. a) Frequency dependence of the imaginary part of the spin susceptibility for the Hubbard model ($U/W = 2.0$, $\delta = 0.05$) at different temperatures T/W; b) temperature dependence of the relaxation rate $1/T_1$ as calculated from equation (2) for different fillings.

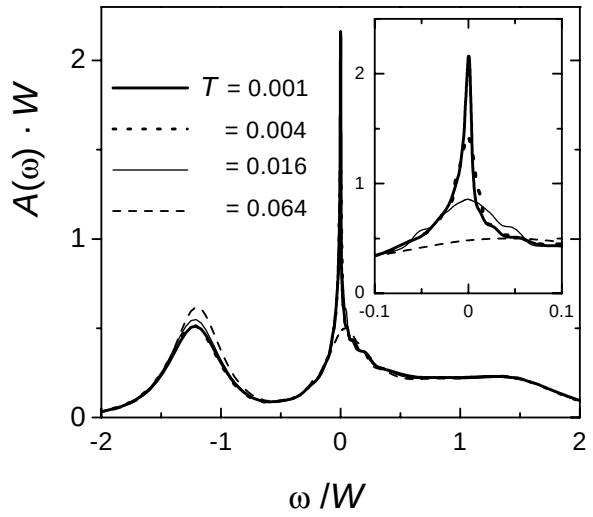

Fig. 5. Temperature dependence of the f spectral function for the periodic Anderson model with on–site hybridization, $U = 2$, $V = 0.5$, $n_f \approx 1$, and $n_c \approx 0.4$. The inset focuses on the quasiparticle peak.

also Fig. 5). This corresponds to a significant change in the entropy of the system within a very small temperature range, corresponding to the large γ-values observed experimentally.

The results for the imaginary part of the spin-susceptibility Im $\chi(\omega, T = 0)$ are shown in Figure 3b for the same set of parameters. For small frequencies, the imaginary part is linear in ω with a slope which is proportional to $(m^*)^2$. Im $\chi(\omega, T = 0)$ shows a maximum at a frequency ω^* which is proportional to $(m^*)^{-1}$. The frequency ω^* can be interpreted as the energy required to break up the singlet which is formed for $T \to 0$.

The calculation of the relaxation rate in equation (2) also requires the temperature dependence of $\chi(\omega, T)$ (see Ref. [51] for technical details of the finite-temperature NRG). Im $\chi(\omega, T)$ is shown in Figure 4a for a fixed filling $\delta = 0.05$. The suppression of the peak in Im $\chi(\omega, T)$ upon increasing temperature is consistent with the loss of spectral weight of the coherent quasiparticle peak in the spectral function (see also Fig. 5). The temperature dependence of the relaxation rate $1/T_1(T)$ is now straightforwardly calculated from equation (2) and shown in Figure 4b for three different fillings. A temperature scale T^* can now be defined conveniently *via* the maximum in $1/T_1(T)$.

Though we do not attempt to fit these numerical results directly to the experimental data, the overall qualitative agreement with the data available for $Gd_{1-y}Sr_yTiO_3$ is very good.

Let us now turn to the periodic Anderson model as a model for the heavy–fermion formation in Kondo–lattice systems [20]

$$H = \varepsilon_f \sum_{i\sigma} f^\dagger_{i\sigma} f_{i\sigma} + U \sum_i f^\dagger_{i\uparrow} f_{i\uparrow} f^\dagger_{i\downarrow} f_{i\downarrow} + \sum_{k\sigma} \varepsilon_k c^\dagger_{k\sigma} c_{k\sigma} + \sum_{ij\sigma} V_{ij} \left(f^\dagger_{i\sigma} c_{j\sigma} + c^\dagger_{j\sigma} f_{i\sigma} \right). \quad (8)$$

This model describes two sorts of fermionic degrees of freedom, the more localized and strongly correlated f-electrons which are coupled to a free conduction band *via* a hybridization V. Only the f-electrons are subject to a strong local Coulomb repulsion U.

Spectral functions for this model have already been calculated within the DMFT (using the NRG-approach) in reference [53]. Here we show the evolution of the spectral function with increasing temperature for $U = 2$, $V = 0.5$, $n_f \approx 1$, and $n_c \approx 0.4$ (see Fig. 5). On lowering the temperature, a very sharp quasiparticle resonance develops in the f spectral function with a width of the order of the low-energy scale $T^* \approx 0.01$.

The general features in the spectral functions are very similar in both the Hubbard model and the periodic Anderson model. The low-energy physics, in particular, is described by a quasiparticle peak which is gradually suppressed upon increasing temperature. We therefore expect the temperature and frequency dependence of the dynamic spin susceptibility to be similar in both models as well. This is indeed the case as has been shown in reference [54]. The temperature dependence of $1/T_1$ exhibits a linear increase for small T and a maximum at a characteristic temperature scale T^*. The high–temperature regime,

however, shows some nonuniversal behaviour, consistent with the experimental observation.

The low-temperature physics in both Hubbard model and periodic Anderson model is that of the screening of local moments, a screening which is perfect in the limit of $T \to 0$. This screening occurs below a certain temperature scale T^*. It does not, however, imply the existence of fully developed moments at higher temperatures, because the screening occurs both for small and large values of U. Nor does it depend on whether the spin-degrees of freedom are localized or not. This is clearly seen in the case of the Hubbard model where the same electronic degrees of freedom are responsible for transport and spin dynamics.

4 Summary

We discussed heavy–fermion formation as observed in transition–metal oxides and in transition metals and compared the results to those observed in $4f$– and $5f$–derived heavy–fermion compounds. We specifically focused on dynamical aspects and presented results of the dynamic susceptibility as probed in ESR and NMR experiments *via* the temperature dependence of linewidth (ESR) and spin–lattice relaxation rate (NMR). And while it is clear, that in $4f$– and $5f$–derived heavy–fermion compounds the Kondo effect gives the essentials of the underlying physics, the routes to heavy fermions are certainly very different in the case of transition–metal oxides and transition metals. Magnetic frustration, or the closeness to either a metal–to–insulator transition or a quantum critical point are discussed as possible scenarios. For LiV_2O_4, even the Kondo effect has been discussed as a possible origin for the appearance of heavy quasiparticles. The calculation of the dynamic susceptibility is carried out in the framework of the Hubbard model and of the periodic Anderson model, respectively. In both models a narrow quasiparticle peak appears at low temperatures and energies resulting in strongly enhanced effective masses. It documents that s–f on–site hybridization like in the periodic Anderson model and electronic correlations in systems close to half conduction–band filling like in the Hubbard model yield similar spectral densities and similar dynamic susceptibilities. In the calculations for the Hubbard model, the temperature dependence of the relaxation rate shows a very similar behaviour upon doping as in the experiments on $Gd_{1-y}Sr_yTiO_3$. This opens the possibility of a qualitative (or even quantitative) understanding of ESR and NMR measurements within calculations based on a microscopic model — in contrast to phenomenological fits which have been almost exclusively used in the literature so far. To describe the dynamic susceptibilities in frustrated magnets, so far phenomenological spin–fluctuation theories have to be utilized. Microscopic models still have to be developed.

This work was supported by the Deutsche Forschungsgemeinschaft *via* the Sonderforschungsbereich 484 *Kooperative Phänomene im Festkörper: Metall–Isolator–Übergänge und Ordnung mikroskopischer Freiheitsgrade*, Augsburg and partly by the Bundesministerium für Bildung und Forschung (BMBF) under the contract number EKM 13N6917.

References

1. K. Andres, J.E. Graebner, H.R. Ott, Phys. Rev. Lett. **35**, 1779 (1975)
2. F. Steglich, J. Aarts, C.D. Bredl, W. Lieke, D. Meschede, W. Franz, H. Schäfer, Phys. Rev. Lett. **43**, 1892 (1979)
3. H. Wada, H. Nakamura, E. Fukami, K. Yoshimura, M. Shiga, Y. Nakamura, J. Magn. Magn. Mater. **70**, 17 (1987); M. Shiga, K. Fujisawa, H. Wada, J. Phys. Soc. Jpn **62**, 1329 (1993)
4. R. Ballou, E. Lelièvre-Berna, B. Fåk, Phys. Rev. Lett. **76**, 2125 (1996); C. Lacroix, B. Canals, J. Magn. Magn. Mater. **196-197**, 622 (1999)
5. S. Kondo, D.C. Johnston, C.A. Swenson, F. Borsa, A.V. Mahajan, L.L. Miller, T. Gu, A.I. Goldman, M.B. Maple, D.A. Gajewski, E.J. Freeman, N.R. Dilley, J. Merrin, K. Kojima, G.M. Luke, Y.J. Uemura, O. Chmaissem, J.D. Jorgensen, Phys. Rev. Lett. **78**, 3729 (1997)
6. C. Urano, M. Nohara, S. Kondo, F. Sakai, H. Takagi, T. Shiraki, T. Okubo, Phys. Rev. Lett. **85**, 1052 (2000)
7. H. Kaps, M. Brando, W. Trinkl, N. Büttgen, A. Loidl, E.W. Scheidt, M. Klemm, S. Horn, J. Phys.: Cond. Matt. **13**, 8497 (2001); M. Brando, N. Büttgen, V. Fritsch, J. Hemberger, H. Kaps, H.-A. Krug von Nidda, M. Nicklas, K. Pucher, W. Trinkl, A. Loidl, E.-W. Scheidt, M. Klemm, S. Horn, Eur. Phys. J. B **25**, 289 (2002)
8. K. Kadowaki, S.B. Woods, Solid State Commun. **58**, 507 (1986)
9. K.G. Wilson, Rev. Mod. Phys. **47**, 773 (1975)
10. H.R. Ott, Prog. Low Temp. Phys. **11**, 215 (1987)
11. P. Fulde, Ann. Phys. **9**, 871 (2000)
12. D. Vollhardt, Rev. Mod. Phys. **56**, 99 (1984)
13. A. Georges, G. Kotliar, W. Krauth, M.J. Rozenberg, Rev. Mod. Phys. **68**, 13 (1996)
14. G.R. Stewart, Rev. Mod. Phys. **56**, 755 (1984)
15. N. Grewe, F. Steglich, *Handbook of the Physics and Chemistry of Rare Earths*, Vol. 14, edited by K.A. Gschneidner Jr., L. Eyring (Elsevier, 1991), p. 343
16. M. Loewenhaupt, K.H. Fischer in *Handbook of the Physics and Chemistry of Rare Earths*, Vol. 16, edited by K.A. Gschneidner Jr., L. Eyring (Elsevier, 1993), p. 1; E. Holland-Moritz, G.H. Lander, *Handbook of the Physics and Chemistry of Rare Earths*, Vol. 19, edited by K.A. Gschneidner Jr., L. Eyring (Elsevier, 1994), p. 1
17. For an early review on the NMR work see K. Asayama, Y. Kitaoka, Y. Kohori, J. Magn. Magn. Mater. **76 & 77**, 449 (1988); E. Dormann in *Handbook of the Physics and Chemistry of Rare Earths*, Vol. 14, edited by K.A. Gschneidner Jr., L. Eyring (Elsevier, 1991), p. 63
18. B. Elschner, A. Loidl, in *Handbook of the Physics and Chemistry of Rare Earths*, Vol. 14, edited by K.A. Gschneidner Jr., L. Eyring (Elsevier, 1997), p. 221; H.-A. Krug von Nidda, M. Heinrich, A. Loidl, in *Relaxation Phenomena: Liquid Crystals, Magnetic Systems, Polymers, High-Tc Superconductors, Metallic Glasses*, edited by W. Haase, S. Wrobel (Springer, Berlin-Heidelberg-New York, 2003), p.112
19. N. Büttgen, R. Böhmer, A. Krimmel, A. Loidl, Phys. Rev. B **53**, 5557 (1996); H.-A. Krug von Nidda, A. Schütz, M. Heil, B. Elschner, A. Loidl, Phys. Rev. B **57**, 14344 (1998)

20. A.C. Hewson, *The Kondo Problem to Heavy Fermions* (Cambridge Univ. Press, Cambridge 1993)
21. D.L. Cox, N.E. Bickers, J.W. Wilkens, J. Appl. Phys. **57**, 3166 (1985)
22. M. Heinrich, H.-A. Krug von Nidda, V. Fritsch, A. Loidl, Phys. Rev. B **63**, 193103 (2001)
23. M.J. Lysak, D.E. MacLaughlin, Phys. Rev. B **31**, 6963 (1985); M. Coldea, H. Schäffer, V. Weissenberger, B. Elschner, Z. Physik B: Cond. Matt. **68**, 25 (1987)
24. N. Büttgen, H.-A. Krug von Nidda, A. Loidl, Physica B **230-232**, 590 (1997); H.-A. Krug von Nidda, A. Schütz, M. Heil, B. Elschner, A. Loidl, Appl. Magn. Reson. **12**, 287 (1997)
25. T. Moriya, J. Magn. Magn. Mater. **14**, 1 (1979)
26. A. Ishigaki, T. Moriya, J. Phys. Soc. Jpn **65**, 3402 (1996)
27. K. Kumagai, T. Suzuki, Y. Taguchi, Y. Okada, Y. Fujishima, Y. Tokura, Phys. Rev. B **48**, 7636 (1993)
28. K. Yoshimura, T. Imai, T. Kiyama, K.R. Thurber, A.W. Hunt, K. Kosuge, Phys. Rev. Lett. **83**, 4397 (1999)
29. S.T.Bramwell, M.J.P. Gingras, Science **294**, 1495 (2001)
30. V.I. Anisimov, M.A. Korotin, M. Zölfl, Th. Pruschke, K. Le Hur, T.M. Rice, Phys. Rev. Lett. **83**, 364 (1999); I.A. Nekrasov, Z.V. Pchelkina, G. Keller, Th. Pruschke, K. Held, A. Krimmel, D. Vollhardt, V.I. Anisimov, Phys. Rev. B **67**, 085111 (2003)
31. V. Eyert, K.-H. Höck, S. Horn, A. Loidl, S. Riseborough, Europhys. Lett. **46**, 762 (1999)
32. A. Krimmel, A. Loidl, M. Klemm, S. Horn, H. Schober, Phys. Rev. Lett. **82**, 2919 (1999)
33. P. Fulde, A.N. Yaresko, A.A. Zvyagin, Y. Grin, Europhys. Lett. **54**, 779 (2001)
34. C. Lacroix, Can. J. Phys. **79**, 1469 (2001)
35. M.S. Laad, L. Craco, E. Müller-Hartmann, Phys. Rev. B **67**, 033105 (2003)
36. S. Burdin, D.R. Grempel, A. Georges, Phys. Rev. B **66**, 045111 (2002)
37. H. Nakamura, K. Yoshimoto, M. Shiga, M. Nishi, K. Kakurai, J. Phys.: Cond. Matt. **9**, 4701 (1997)
38. N. Fujiwara, Y. Ueda, H. Yasuoka, Physica B **237-238**, 59 (1997); N. Fujiwara, H. Yasuoka, Y. Ueda, Phys. Rev. B **57**, 3539 (1998)
39. Y. Kohori, Y. Noguchi, T. Kohara, J. Phys. Soc. Jpn **62**, 447 (1993)
40. J.R. Stewart, B.D. Rainford, R.S. Eccleston, R. Cywinski, Phys. Rev. Lett. **89**, 186403 (2002)
41. G. Cao, S. McCall, M. Shepard, J.E. Crow, R.P. Guertin, Phys. Rev. B **56**, 321 (1997)
42. Y. Maeno, H. Hashimoto, K. Yoshida, S. Nishizaki, T. Fujita, J.G. Bednorz, F. Lichtenberg, Nature **372**, 532 (1994); Y. Maeno, T.M. Rice, M. Sigrist, Phys. Today **54**, 42 (2001)
43. Y. Maeno, K. Yoshida, H. Hashimoto, S. Nishizaki, S. Ikeda, M. Nohara, T. Fujita, A.P. Mackenzie, N.E. Hussey, J.G. Bednorz, F. Lichtenberg, J. Phys. Soc. Jpn **66**, 1405 (1997
44. T. Imai, A.W. Hunt, K.R. Thurber, F.C. Chou, Phys. Rev. Lett. **81**, 3006 (1998)
45. M. Minakata, Y. Maeno, Phys. Rev. B **63**, 180504 (R) (2001); K. Pucher, J. Hemberger, F. Mayr, V. Fritsch, A. Loidl, E.-W. Scheidt, S. Klimm, R. Horny, S. Horn, S.G. Ebbinghaus, A. Reller, R.J. Cava, Phys. Rev. B **65**, 104523 (2002)
46. A. Liebsch, Europhys. Lett. **63**, 97 (2003)
47. J. Hubbard, Proc. R. Soc. London A **276**, 238 (1963); M. C. Gutzwiller, Phys. Rev. Lett. **10**, 159 (1963); J. Kanamori, Prog. Theor. Phys. **30**, 275 (1963)
48. W. Metzner, D. Vollhardt, Phys. Rev. Lett. **62**, 324 (1989)
49. H.R. Krishna-murthy, J.W. Wilkins, K.G. Wilson, Phys. Rev. B **21**, 1003 (1980); *ibid.* **21**, 1044 (1980)
50. R. Bulla, A.C. Hewson, Th. Pruschke, J. Phys.: Cond. Matt. **10**, 8365 (1998)
51. R. Bulla, T.A. Costi, D. Vollhardt, Phys. Rev. B **64**, 045103 (2001)
52. M. Jarrell, Th. Pruschke, Phys. Rev. B **49**, 1458 (1994)
53. Th. Pruschke, R. Bulla, M. Jarrell, Phys. Rev. B **61**, 12799 (2000)
54. T.A. Costi, N. Manini, J. Low Temp. Phys. **126**, 835 (2002); the Kondo model is considered here which has the same low-temperature physics as the periodic Anderson model